Choosing an Optimum Large Signal Model for GaAs MESFETs and HEMTs

Monte Miller*, Mike Golio*, Bill Beckwith*, Eric Arnold*
Dave Halchin**, Scott Ageno**, Steve Dorn**

*Motorola Strategic Electronics Division
Chandler, AZ 85248-2899
**Motorola Phoenix Corporate Research Laboratories
Tempe, AZ 85283

Abstract - Seven large signal MESFET models and three newly developed HEMT models have been compared, providing the microwave circuit designer with a practical benchmark. The error for each model is quantified and minimized using a modified Newton's method with the restricted step technique of Levenberg and Marquardt. This minimum obtainable error is used as a basis for comparing the models. The validity of this approach is confirmed by comparing predicted to measured large-signal performance made on a Triquint 0.5 µm gate length MESFET. The model comparison tool has also been utilized to develop a general approach to large signal HEMT modeling for circuit simulation applications. A 0.7 µm gate length pseudomorphic HEMT device was used for this portion of the study.

I. Introduction

Choosing a large signal model that provides sufficient accuracy in the prediction of device characteristics can be a problem for the microwave engineer. Several versions of large signal circuit simulation programs exist, many offering a choice of MESFET models. The process of determining ideal model parameters and evaluating the ultimate potential of the models, however, can be difficult. The problem is more difficult for HEMT applications, since accurate large signal models for these devices are not commonly available.

Six empirical MESFET models and one physically based model have been incorporated into a newly developed, parameter extraction program. In addition, three empirical HEMT models have been developed and incorporated into the same extraction routines. The parameter extraction program determines the model parameters which provide optimum performance predictions from each model.

The MESFET models compared are:

- •Model 1- The model proposed by Curtice and Ettenberg [3].
- •Model 2- The hyperbolic tangent model presented by Curtice, modified by Meta-Software [4],[5].
- •Model 3- The physically based model originally proposed by Lehovec and Zuleeg, modified by Hartgring and Golio [6], [7],[8].
- •Model 4- The model proposed by Materka and Kacprzak [9].
- •Model 5- The model proposed by Statz, et al., [10].
- •Model 6- The model proposed by Curtice [4].
- •Model 7- The model proposed by Statz, et al., modified by Triquint Semiconductor [11].

The three HEMT models are obtained by applying a newly developed general modification procedure to existing MESFET models. The models used for this portion of the study are:

- •Model 8- Model 6 with additional HEMT parameters.
- •Model 9- Model 4 with additional HEMT parameters.
- •Model 10- Model 2 with additional HEMT parameters.

The parameter extraction program uses two methods to optimize the parameters contained in the model equations. A constrained random optimization is used first, followed by the Levenberg-Marquardt method [1],[2]. The use of a random technique enables the Levenberg-Marquardt optimization to begin from a new starting point each time the extraction program is executed, thus addressing the problem of entrapment in local minima.

The model equations for drain current are incorporated into the extraction program for each model. The derivatives for Ids with respect to Vgs and Vds are expressed analytically to determine the equations for transconductance and output conductance respectively. These expressions are also incorporated into the extraction program. The model equations for the device capacitances are not included in this comparison. To obtain capacitance parameters for the full large signal prediction comparisons, a random optimization routine has been used. For most large signal models and for all of the models considered in this investigation, the extraction of capacitance-voltage parameters is independent of the extraction of other model parameters.

II. Optimization of Model Parameters

The parameter extraction program was developed to solve the non-linear optimization problem involved in device modeling. The problem of optimization is to adjust the model parameters in the device model equation to improve the fit between measured and modeled data. This is accomplished by optimizing a uniquely defined objective function. The objective function chosen for this work measures the error in the DC as well as the AC characteristics of the device. Our objective function is termed Error Magnitude Unit or EMU and is defined as

$$EMU = \frac{EMU'}{3n} \quad (1)$$

where:

n = Number of bias points

$$EMU' = \sum_{i=1}^{n} (E_{Ids}(i)WF_{Ids} + E_{gm}(i)WF_{gm} + E_{Gds}(i)WF_{Gds})100$$

and

$$E_{xxx}(i) = \frac{(Meas(i)-Mod(i))^2}{Meas(i)^2}$$

WF_{Ids}, WF_{gm}, WF_{Gds} are normalized weighting factors.

The AC characteristics are described by fitting the modeled transconductance and output conductance to measured values of microwave transconductance and output conductance. These values of gm and Gds are obtained using a modified technique proposed by Arnold, et al. [12]. Development of the

CH2848-0/90/0000-1279$01.00 © 1990 IEEE

nonlinear model is based on the bias dependence of the small-signal device characteristics. The method of predicting nonlinear behavior of MESFETs by determining the bias and frequency dependence of s-parameters was proposed by Willing, et al. [13]. S-parameters are measured for discrete combinations of bias voltages. Values for Vds are chosen to characterize the bias dependence of the device in both the linear and saturation regions. Values for Vgs are chosen to characterize the device from 0.0 Volts through pinch-off. A small-signal model including the parasitic resistances and inductances is used to extract the model element values from the measured s-parameters.

The measured DC current characteristics are also used in the extraction. This behavior is represented by the original device equation for Ids.

This technique eliminates the need for time-consuming transient or harmonic measurements. Likewise, large amounts of data are compressed which further simplifies the extraction process.

In addition to the large signal extraction program, both the characterization and small-signal equivalent element determination have been automated to minimize the cycle time from device to large signal model. Once measurements and small signal model determination are complete, required parameters for most models are extracted using this program on an AT class computer in less than 15 minutes. The current time required to characterize, determine small signal equivalent circuit element values and parameter extract is approximately 2-4 hours.

In order to test the robustness of this approach, each individual parameter of Model 2 was perturbed by ± 20 to ± 50 percent of an optimum value followed by the parameter extractor being restarted. This determined whether or not the parameters were converging to a unique solution. The Levenberg-Marquardt optimization process was allowed to terminate itself, thus determining optimum parameter values. The criteria for termination is established to be when the EMU does not decrease by 0.001 for 3 consecutive iterations. The other parameters were started from the value reached after the random optimization operation. The extractor converged to the same solution for every parameter tested. Another test was performed by examining the relationship between EMU and the individual parameters to determine if the objective function was well behaved in each parameter space. The objective function was found to be smooth and continuous with no observable local minima.

Figures 1, 2, and 3 show the measured and modeled results of DC Ids, rf Gds, and rf gm using this optimization approach with the weighting factors all set to 1.0. The device used in these measurements was a depletion mode rf probeable .5x300 μm MESFET manufactured by Triquint Semiconductor. The parameter extraction was performed for Model 2. The program was allowed to terminate by itself with the criteria for termination being the same as that described above. The EMU for this case is 2.60. Note, that better agreement between measured and modeled characteristics shown in any of the Figures 1-3 can be obtained at the expense of the other two. Exact agreement of all three simultaneously, however, is not possible with the models considered. This limitation of the models is caused by their inability to model the low frequency dispersion of Gds and gm observed in GaAs MESFETs [14].

III. MESFET TEST RESULTS

DC and rf measurements were made on 0.5x300 μm and 1x300 μm devices. S-parameters and DC I-V characteristics were measured at 25 different bias points covering the linear through saturation regions. The parameter extraction program was run using Models 1-7 with all weighting factors set to 1.0. When all 25 data points were used the optimization of model parameters was called global optimization. When only the 10 data points in the saturation region were used the optimization was called local optimization. The program ran until the EMU did not decrease by 0.001 for three consecutive iterations. The program

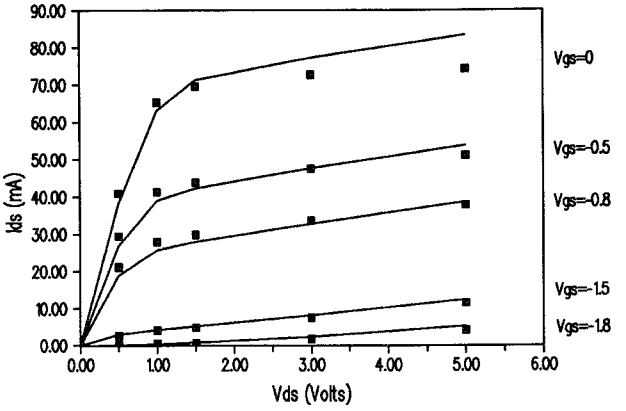

FIGURE 1. A comparison of DC measured and modeled drain-source current vs. drain-source voltage. Blocks are measured for a 0.5x300 μm device while the solid lines are predictions from Model 2 using optimized parameters.

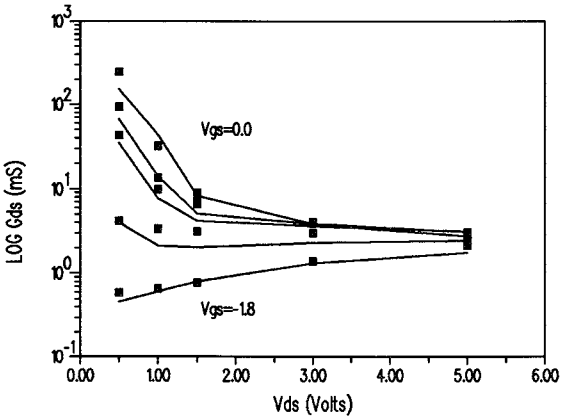

FIGURE 2. A comparison of rf measured and modeled output conductance. Blocks are measured for a 0.5x300 μm device while the solid lines are predictions from Model 2 using optimized parameters.

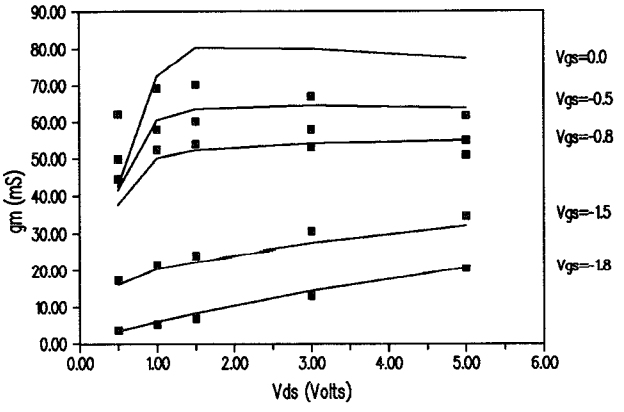

FIGURE 3. A comparison of rf measured and modeled transconductance. Blocks are measured for a 0.5x300 μm device while the solid lines are predictions from Model 2 using optimized parameters.

TABLE I
Final EMU for all seven models in a global and local optimization.

Device	Type of Optimization	Error Magnitude Unit (EMU)						
		MOD1	MOD2	MOD3	MOD4	MOD5	MOD6	MOD7
0.5 x 300 (microns)	Global	273	2.526	22.029	7.782	19.074	19.029	3.314
	Local	21.895	0.395	14.256	2.004	14.433	15.954	0.942
1.0 x 300 (microns)	Global	201	1.374	17.150	5.609	13.580	13.267	2.168
	Local	20.639	0.555	11.798	2.377	11.925	12.733	0.807

was run for each model two to three times with the parameters converging to within 1 percent of each final solution value. Table I lists the models and their final EMU obtained for both a global and local optimization.

Figure 4 is a bar graph illustrating the relative performance of each model for both global and local optimizations for the 0.5 μm device. The general trend is Model 2, Model 7, and Model 4 having substantially better EMU for both a global and local optimization. As expected the EMU obtained for local optimization was better than that obtained for global optimization. This is due to the EMU being calculated for fewer bias points which places less constraints on the model.

Model 1 has serious problems predicting device characteristics when using the global optimization scheme. This is probably associated with the third order polynomial in the model equation. Another irregularity in the data calculated by Model 1 is a tendency to predict non-physical device behavior such as a negative drain current for certain bias voltages. This occurs for both local and global optimization.

A global optimization of Model 2, 5 and 6 was used in a SPICE simulation to predict the fundamental and third harmonic power content of the output signal as a function of the input power. Two tone measurements were made of the fundamental and third harmonic power output as a function

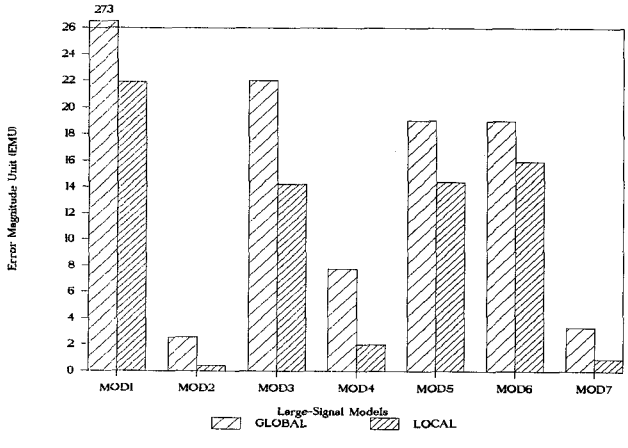

FIGURE 4. Error Magnitude Unit for the various models applied to a 0.5x300 μm device. This illustrates the comparison of minimum obtainable error between measured and modeled data for seven large signal FET models.

of input power. The optimized parameters used in conjunction with the gate diode parameters, parasitic resistances and inductances, and bias dependent capacitance expressions constitute the full large signal model used in these simulations. Figure 5 illustrates the measured data and results of the simulations. All three models show qualitative agreement for the fundamental and third harmonic. Model 2 shows the best agreement followed by Model 5 and 6 respectively. The accuracy of these predictions corresponds exactly to the relative ranking of these models by EMU presented in Figure 4. This

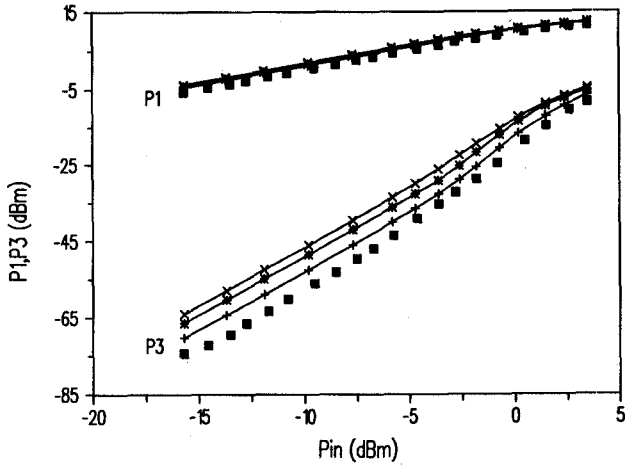

FIGURE 5. Fundamental and third harmonic power vs. input power. The blocks are measured data, plus signs are predicted values using model 2, asterisks are predicted values using model 5 and x's are predicted values using model 6.

correspondence confirms the effectiveness of the method presented earlier to determine the large signal model parameters. Although the EMU for Model 5 is almost identical to that of Model 6, Model 5 shows better agreement to the measured data for both the fundamental and third harmonic frequencies. Curtice [15] found that the inclusion of bias dependent capacitances Cgs and Cgd significantly improves the prediction of the power of both the second and third harmonic frequencies. The bias dependent capacitance expressions for Model 5 are better than those of Model 6 [10]. This is believed to be the reason Model 5 shows a closer fit to the measured data than Model 6. The same trends exist in all three model's ability to simulate third order intercept point.

IV. HEMT MODEL RESULTS

GaAs MESFET models successfully predict large signal performance by predicting voltage dependance of device characteristics. Of the nonlinearities involved in device behavior, transconductance is most critical to the accurate prediction of many important large signal effects. For microwave application, therefore, it is important that large signal models be capable of modeling device transconductance. The differences between the transconductance characteristics of HEMTs and MESFETs is one of the most significant distinctions between the device's electrical behavior. For this reason, we have focused on improving the transconductance predictions of existing FET models.

To accomplish this improved prediction capability, the analytical transconductance expression of existing FET models was modified:

$$g_m = g_{mFET} - f(V_{ds})B(V_{gs} - V_{pf})^m \quad (2)$$

where g_{mFET} is the MESFET model transconductance, $f(V_{ds})$ is the nonlinear correction term, V_{pf} is a voltage where transconductance begins to degrade, and B and m are empirical transconductance degradation parameters. The transconductance as modified by this equation is then integrated with respect to Vgs to derive the I-V characteristics of the model:

$$I_{ds} = \int g_m \, dV_{gs} \quad (3)$$

which can also be expressed in terms of a standard MESFET

current with a modification term introduced by the transconductance degradation term. An expression for output conductance is then derived by taking the derivative of the I-V equation with respect to V_{ds}. These quantities were calculated for 3 standard FET models and implemented in the parameter extractor program.

DC characteristics and s-parameter measurements to 26.5 GHz were made over bias on a 0.7x200 µm pseudomorphic HEMT produced in our laboratory. Parameter extraction was accomplished in a manner identical to that used for the MESFET devices discussed earlier. Both the standard FET models and their associated newly developed HEMT models were used in the extraction exercise.

Figure 6 and 7 present the measured and modeled HEMT DC I-V and transconductance for both model 2 (MESFET model) and model 10 (modified with the HEMT degradation parameters). The improvement in the model predictions when the HEMT terms are added is clearly evident. An EMU value of 3.7 results when model 10 is used to describe the HEMT device behavior. This value compares very favorably with the best EMU values found for the MESFET device models of Table I. Improvements were also made in rf output conductance predictions when the HEMT parameters are added. Similar improvements were realized for the other MESFET models modified using our prescribed technique (models 4 and 6).

V. CONCLUSION

This brief reports the use of both a random and restricted step method of optimization to compare the ability of MESFET and HEMT large signal models to predict device behavior. A unique objective function was used to optimize the drain current equation and its derivatives for both DC and AC characteristics. The extracted models were used to predict the power of the harmonic content of the output signal versus input power with excellent results.

A general modeling strategy which allows MESFET models to be modified to describe HEMT behavior has also been presented. Three models have been produced using this technique. The parameter extraction tool has been demonstrated to be useful in developing these new device models.

REFERENCES

[1] K. Levenberg,"A Method for the solution of certain problems in least squares,"Quart. Appl. Math., vol. 2, pp. 164-168, 1944.

[2] D. Marquardt,"An algorithm for least-squares estimation of nonlinear parameters," *SIAM Journal Appl. Math.*, vol. 11, pp. 431-441, 1963.

[3] W. R. Curtice and M. Ettenberg,"A Nonlinear GaAs FET Model for Use in the Design Of Output Circuits for Power Amplifiers," *IEEE Trans. Microwave Theory Tech.*, vol. MTT-33, pp. 1383-1394, 1985.

[4] W. R. Curtice,"A MESFET Model for Use in the Design of GaAs Integrated Circuits," *IEEE Trans. Microwave Theory Tech.*, vol. MTT-28, pp. 448-456, 1980.

[5] HSPICE User's Manual, (Version H8907), Meta-Software, Campbell, CA 95008, 1989.

[6] K. Lehovec and R. Zuleeg,"Voltage-Current Characterization of GaAs JFETs in the Hot Electron Range," *Solid State Elec.*, vol. 13, pp. 1415-1429, 1970.

[7] C. Hartgring,"Silicon MESFETs,"Phd Thesis, Dept. of Elec. Eng., University of California, Berkeley, June 1981.

[8] J. Michael Golio, et al.,"A Large-signal GaAs MESFET Model Implemented on SPICE," *IEEE Circuits and Devices Mag.*, pp. 21-30, September 1985.

[9] T. Kacprzak and A. Materka,"Compact dc Model of GaAs FET's for Large-Signal Computer Calculation, " *IEEE Journal of Solid-State Circuits*, vol. SC-18, pp. 211-213, April 1983.

[10] H. Statz, et al.,"GaAs FET Device and Circuit Simulation in SPICE," *IEEE Trans. on Elec. Devices*, vol. ED-34, pp. 160-169, 1987.

[11] A. McCamant, D. Smith, G. McCormack, An Improved GaAs MESFET Model for SPICE, submitted for publication, Triquint Semicond. Inc., Beaverton, OR 97076, 1989.

[12] E. Arnold, et al.,"Direct Extraction of GaAs MESFET Intrinsic Element and Parasitic Inductance Values, " *IEEE MTT-S Digest*, 1990.

[13] H. Willing, et al.,"A Technique for Predicting Large-Signal Performance of a GaAs MESFET," *IEEE Trans. Microwave Theory Tech.*, vol. MTT-26, pp. 1017-1023, 1978.

[14] J. Michael Golio, et al.,"Frequency Dependent Electrical Characteristics of GaAs MESFETs, "accepted for publication *IEEE Trans. Elec. Devices*, 1989.

[15] W.R. Curtice,"On-Wafer Verification of a Large-Signal MESFET Model," *IEEE Trans. Microwave Theory Tech.*, vol. MTT-37, pp. 1809-1811, 1989.

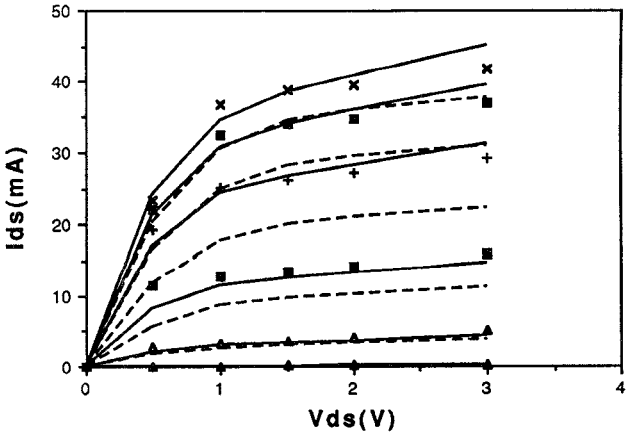

FIGURE 6. Measured and modeled drain-source current vs. Vds. Bias points are Vgs = 0, -0.1, -0.25, -0.5, -0.75,and -1V. Dashed curves are from model 2, solid curve from model 10 and discrete points are measured for 0.7x200 µm HEMT.

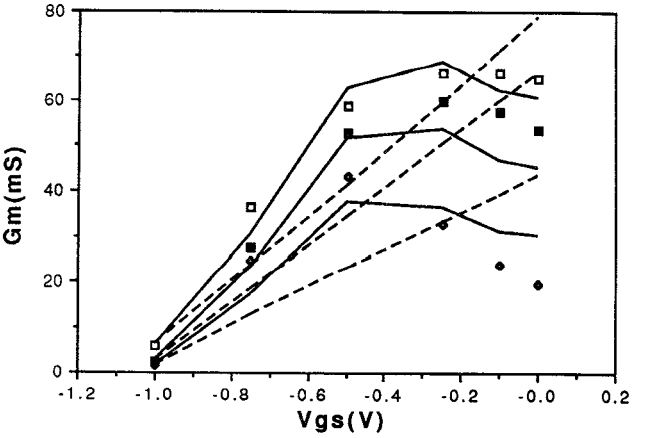

FIGURE 7. Measured and modeled transconductance vs. Vgs. Bias points are Vds = 0.5, 1, and 3 V. Dashed curves are from model 2, solid curve from model 10 and discrete points are measured for 0.7x200 µm HEMT.